Stockpile Stewardship Quarterly

Defense Programs | *Stockpile Stewardship in Action* | Volume 2, Number 1

Message from the Assistant Deputy Administrator for Stockpile Stewardship, Chris Deeney

At the recent SSAA Symposium, Dr. Donald L. Cook, the NNSA Deputy Administrator for Defense Programs, challenged us all with his talk: *It's Not Your Grandfather's Deterrent*. This should be a rallying cry for the science, technology and engineering (ST&E) community to ensure that it is not our grandfathers' deterrent.

Our stockpile will undergo a significant modernization in the next decade, and our ST&E community must deliver the science and technologies that will ensure Dr. Cook is correct. This will be achieved by both excellent ST&E plus a commitment and drive to insert these advances into our assessment process and modernized systems. To facilitate this, we have listed the Technology Readiness Levels (see page 10). This level structure rigorously allows an assessment of where technology is in the development process. We encourage all of you in the ST&E development process to use it to execute your development paths. Familiarity with these levels will also allow you to have clearer discussions with your colleagues in product realization teams. ST&E *is* stockpile modernization: We must live this truth.

As ever, the challenge of stockpile stewardship and supporting national nuclear security drives us to push the state-of-the-art. In this issue, we have great examples of work being done from mix in plasmas at a microscopic scale to mix in fallout planes. In addition, our ability to compress and diagnose materials at relevant conditions continues to improve (Fernsen et al., Armentrout, and Brown). While discussing our grandparents, the article on microscopic fission theory really shows how in a critical area to stewardship, modern tools are addressing a 75-year-old challenge identified by the great pioneers in nuclear science.

Thank you, again, to the NNSA and ORISE teams that put on the SSAA Symposium and administered the solicitations. The program continues to excel, and the quality of the work and people is amazing.

In Remembrance

Dr. Dillon Heierman McDaniel, 1945-2012

It is with deep admiration and affection that we remember Dr. Dillon McDaniel, an esteemed member of the international high energy density physics community, who passed away on May 1, 2012.

Dillon received his B.S. and Ph.D. degrees in physics from the University of Texas at Austin. Right out of graduate school, he went to work as a research scientist in the Pulsed Power Program at Sandia National Laboratories (SNL). His career at SNL would include a succession of supervisory and managerial roles for z-pinch research and x-ray generation sources, including collaboration with Russian and French programs and the Defense Threat Reduction Agency, and go on to span 38 years. In 2004, Dillon became a SNL Senior Scientist in the areas of inertial confinement fusion, high energy density physics, shock physics and x-ray source applications of pulsed power. In 2009, Dillon came to NNSA Headquarters as a detailee from SNL and we had the pleasure of working closely with him. We extend our condolences to his family. We shall miss our friend and colleague.

Inside this Issue

Comments

Questions or comments regarding the *Stockpile Stewardship Quarterly* should be directed to Terri.Batuyong@nnsa.doe.gov

Technical Editor: Dr. Chris Werner, Publication Editor: Millicent Mischo

Los Alamos National Laboratory (LANL) and Argonne National Laboratory (ANL) Complete Groundbreaking Shock Experiments at the Advanced Photon Source (APS)

by Brian J. Jensen, S.N. Luo, and D. Hooks (Los Alamos National Laboratory)

For decades, scientists have studied shock waves and how they propagate through a material[1] to learn how materials fail or break, to understand how materials transform from one phase to another (melting, freezing, etc.), or to generate conditions that are comparable to those found inside the planets. A shock wave (or compression wave) is formed when a projectile impacts a material creating high-pressure states in very short timescales, typically within a few nanoseconds or billionths of a second. These extreme states of matter, found in nature as meteorite impacts or within the earth's core for example, can be created in the laboratory using explosives, lasers, pulsed power and gun systems.

Although there has been much success in relating the shock-wave profile to the material response, standard experimental methods have difficulty when the processes and/or materials are heterogeneous. More advanced diagnostics are required to study complex materials such as foams, powders, high explosives, and complicated processes such as hot-spot formation in explosives or formation of jets from metal surfaces. Developments in synchrotron facilities[2] (intense and coherent x-ray sources) and in detection methods[3,4] provide unique opportunities for ultrafast, high-resolution, spatially resolved measurements to examine materials during impact loading.

To take advantage of synchrotron facilities for shock experiments, a team from LANL in collaboration with scientists from ANL developed a mobile plate impact facility specifically for use at synchrotron sources to perform ultrafast measurements of material subjected to impact loading. The Impact System for Ultrafast Synchrotron Experiments (IMPULSE) is a 12-mm gun system capable of reaching moderate projectile velocities up to approximately 1 km/s. In October 2011, this team completed its first experimental run at the APS. Figure 1 shows photos of the IMPULSE system inside the experimental beamline 32 ID-B at the APS.

Two experimental methods were used to examine shocked materials: phase contrast imaging (PCI) and dynamic Laue diffraction. Figure 2 shows a diagram of the experimental configurations. PCI can be used to obtain high-resolution images with high contrast allowing one to resolve fine features/structures such as cracks, particles, interfaces, etc. Briefly, x-rays transmitted through the samples were converted to visible light (using a scintillator), and imaged onto a fast detector (i.e., a scintillator-to-sample distance optimized for the best contrast) to obtain a detailed 2D image of the event in real time. The second method, Laue diffraction, provides information on a material's atomic structure to diagnose the phase of the material and to examine microscopic defects inside the sample. These diagnostics were used to examine various materials impacted by projectiles using the IMPULSE gun system that was inserted into the x-ray beam. The team successfully performed over 30 experiments on various materials to examine phenomena, including jet formation in cerium metal, dynamic compaction of borosilicate spheres, and

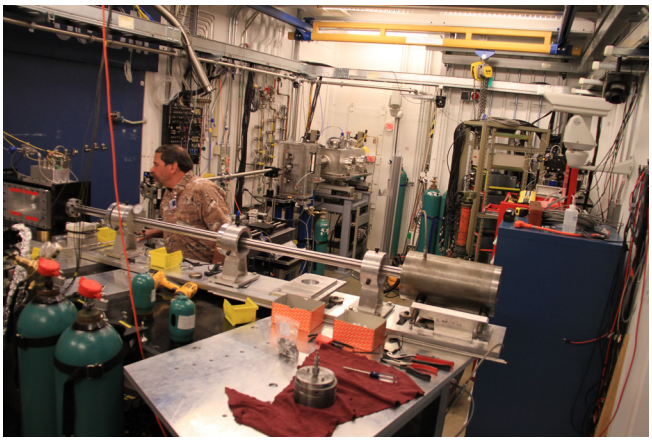

Figure 1. The IMPULSE mini-gun system (12-mm bore) shown inside the experimental hutch at Sector 32 ID-B.

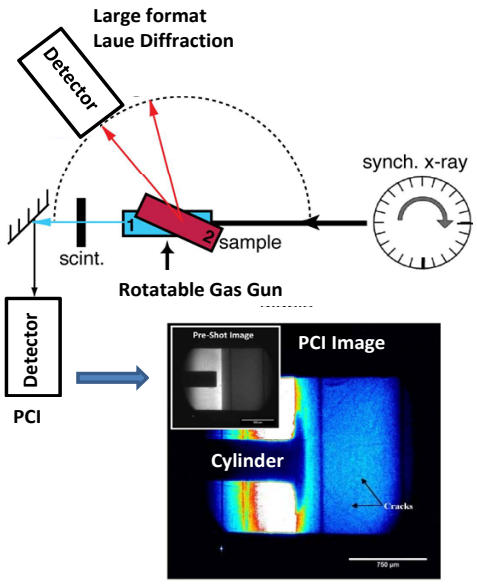

Figure 2. A diagram of phase contrast imaging and dynamic Laue diffraction experiment along with an example image obtained from an experiment that impacted a 300-micron steel cylinder onto a boron carbide plate. The image was taken approximately 500 ns after impact.

high strain-rate impact of steel cylinders onto various target materials. Additional tests were performed using a new three-frame silicon-complementary metal-oxide-semiconductor (CMOS) detector to obtain "shock movies." The team also successfully performed the first impact experiment to obtain dynamic Laue diffraction data (<53 ns) from an iron single crystal. Example PCI data are shown in Figure 2 for a steel cylinder impacting a boron carbide plate.

These dynamic experiments using the phase contrast imaging diagnostic with a single 60-ps width x-ray bunch were groundbreaking. The 3-μm spatially resolved measurements reveal novel phenomena with the possibility of studying the rich underlying physics for materials subjected to high strain rate loading.

"We have firmly established the dynamic phase contrast imaging technique at APS (Section 32 ID-B), with a single x-ray bunch from the standard mode (24-bunch)," said Shengnian Luo from LANL. "The preliminary experiments on dynamic Laue diffraction also showed promise for future success." This work is an important step in the development of future facilities such as the Matter-Radiation Interactions in Extremes (MaRIE)-LANL's signature experimental facility concept and the Dynamic Compression Sector experimental facility proposed to be built at the APS.

This was a collaborative effort between scientists and technicians from LANL's Physics Division (S. Luo, K. Kwiatkowski, and T. Shimada), the Shock & Detonation Physics Group (B. Jensen, J. Esparza, C. Owens, D. Hooks, K. Ramos, J. Yeager, D. Fredenburg, T. Pierce, and R. Saavedra), and the Weapons Test Engineering Group (R. Valdiviez); and ANL (K. Fezzaa and A. Deriy).

References

[1]Marc A. Meyers, Dynamic Properties of Materials (Wiley, New York, 1994).

[2]Q. Shen, W. Lee, K. Fezzaa, Y.S. Chu, F. Carlo et al., Nuclear Instruments and Methods in Physics Research: Section A 582, 77 (2007).

[3]S.W. Wilkins, T.E. Gureyev, D. Gao, A. Pogany, and A.W. Stevenson, Nature 384, 335 (1996).

[4]Y. Wang, X. Liu, K.S. Im, W.K. Lee, K. Fezzaa et al., Nat. Phys. 4, 305 (2008).

Characterization of Activity-Size-Distribution of Nuclear Fallout

by Gregory D. Spriggs, Kim B. Knight, and Richard C. Gostic (Lawrence Livermore National Laboratory)

Understanding the distribution of radioactivity as a function of particle size (here, the activity-size distribution or ASD) of nuclear fallout is one of the most important parameters in the prediction of local fallout. This relationship, unfortunately, remains one of the most elusive topics in the area of nuclear fallout technology largely because the basic, underlying physics of the formation of fallout particles is very complicated and not fully understood. Considerable effort has been made to calculate the ASDs from first principles, but theoretical models have failed to produce results that correlate well with measured, empirical data, and have thus been largely abandoned. Without a viable theoretical model, most nuclear fallout codes rely on empirically determined ASDs based on data collected at the Nevada National Security Site (NNSS) and the Pacific Proving Grounds (PPG). It is common consensus amongst nuclear fallout experts, however, that these empirical ASDs will not work well when trying to predict nuclear fallout in other environments.

Urban environments are a case of considerable interest to many of our government organizations that have some role in preparing for and responding to nuclear terrorism emergencies. Experiments performed at Sandia National Laboratories with conventional explosives detonated over both loose, desert soils and large, dust-free steel plates have shown significant differences in cloud behavior and particle-size formulation. Similar differences were observed at NNSS during the Double Track and Project 57 experiments. Based on these types of measurements, it is surmised that a detonation over an asphalt or concrete surface will not behave the same as a detonation at NNSS. Our inability to predict nuclear fallout in an urban environment represents a major gap in our nuclear fallout technology that needs to be rectified. The only method available for filling this gap is through the development of first-principle, theoretical models that are not only capable of reproducing the historical data from the diversity of tests conducted at NNSS and PPG, but also are general enough to correctly predict the ASD in more complex and less explored environments.

New Research

Spriggs (2008) postulated a new theoretical model for ASDs based on a simple physical process that occurs in the fireball during the cooling phase. This model is referred to as the 1/d model, where d is the physical diameter of any solid particle drawn into the fireball shortly after a detonation. The basic assumption used to formulate this model is simple: When a nuclear detonation occurs close to the surface, the soil in the vicinity of ground zero is drawn up into the fireball. While some of the initial amount of incoming soil is vaporized, most of the incoming particles remain intact and act as condensation sites for the hot vapors within the fireball. If it is assumed that this vapor condenses uniformly over the available surface areas of the incoming soil particles, it can be shown that the specific activity (i.e., curies per gram of substrate) of the fallout is inversely proportional to the grain diameter (1/d). Thus, the initial activity distribution of the cloud forming during any given detonation in any given environment can be calculated if the mass distribution as a function of grain size (i.e., the particle-size distribution or PSD) of the solid material drawn into the fireball is known.

The above process is complicated somewhat by the fact that the PSD in the cloud can change dramatically as a function of time. During the early stages of the cloud rise, the upward draft of the cloud is strong enough to entrain the entire PSD of the soil found at the ground zero, which may include a significant fraction of gravel and large rocks. Because refractory material in the bomb debris vapor condenses first, the ASD formed during this early stage will correspond to the area-distribution of the entire native PSD of the soil in the vicinity of ground zero. During the later stages of the cloud rise, however, the upward draft of the cloud will slow down considerably, and the heavier particles will rapidly settle out, leaving behind the lighter portion of the native PSD. As the cloud continues to cool, the volatile material in the bomb debris vapor begins to condense. The ASD formed during this cooling stage will correspond to the area-distribution of this late-stage PSD, which is depleted of the heavier particles. As a consequence of this rapid change in PSD during the cooling phase, the composition of the radioactive material on the heavier fallout particles is different than the composition found on the smaller particles (a process known as fractionation).

Despite the added complexities introduced by fractionation, the specific activity of the refractory particles and the volatile particles still appear to follow the 1/d model.

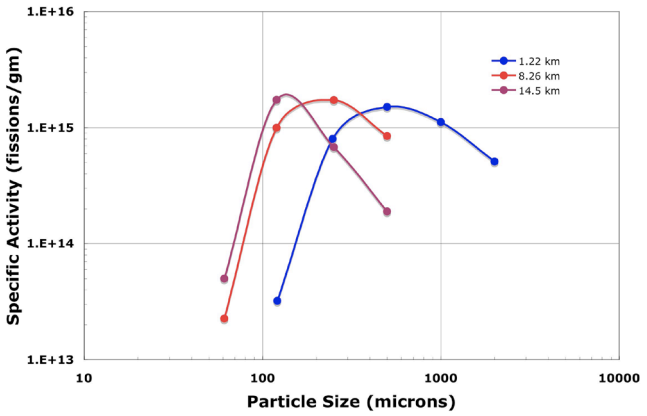

Figure 1. Measured specific activity (expressed as the number of fissions per gram as opposed to curies per gram) of fallout particles for Small Boy. Note that the farther downrange, the smaller the mean particle size. As expected, the tail of each curve follows, to a first approximation, a 1/d dependence.

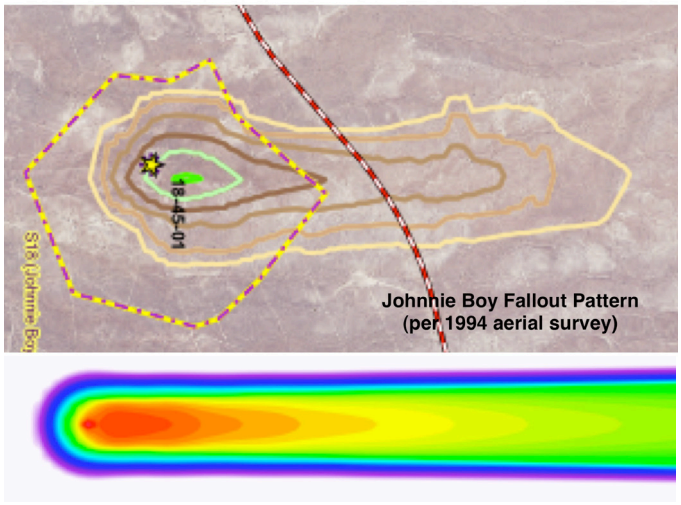

Figure 2. Scaled comparison of the measured (top) and predicted (bottom) fallout pattern for Johnie Boy using the 1/d model. Note that the largest exposure rate occurs somewhat downwind of ground zero. This pattern could not be produced using the same ASD that was predicted for Small Boy and vice versa.

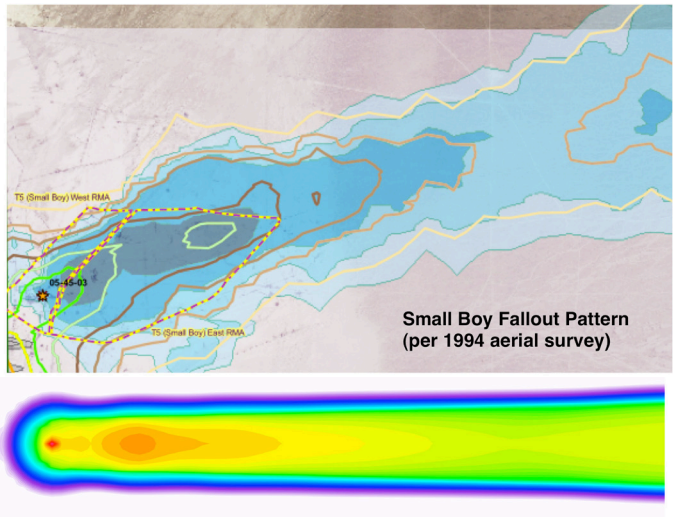

Figure 3. Scaled comparison of the measured (top) and predicted (bottom) fallout pattern for Small Boy using the 1/d model. This model prediction was produced using constant winds since the new fallout code does not yet have complex weather capability. As can be observed, there are two hotspots downwind of ground zero. This fallout pattern could only be produced using the ASD calculated from the measured PSD of the soil at ground zero of Small Boy.

For example, the specific activity of the fallout particles produced during the Small Boy shot showed the 1/d dependence (on the tail of the distribution) at both near-range and far-range locations (see Figure 1). Presumably, the near-range particles were mostly refractory particles and the far-range particles were mostly volatile particles. They separated naturally due to differences in their settling rates: heavier, refractory particles fell in close to ground zero while the lighter, volatile particles fell much farther out.

To further test the 1/d model, we collected and analyzed soil samples from two different low-yield, surface shots at NNSS. Small Boy was detonated in Area 5, which is a dried-up lakebed comprised of very small particles mostly in the form of clays and silts. Johnie Boy was detonated in Area 18, where soil is comprised of relatively larger particles mostly in the form of medium- and coarse-grain sands and gravel. Using a newly developed fallout code that implements the 1/d model, the fallout patterns produced by detonations over these two different soil types were compared to their measured fallout patterns. As can be observed in Figure 2, the predicted fallout pattern is in excellent agreement with the classic teardrop pattern that was measured for Johnie Boy. As can be observed in Figure 3, the predicted fallout pattern for Small Boy is also in agreement with the more complicated fallout pattern that shows two hotspots downwind of ground zero. This type of agreement between model and measurement for both shots could not have been obtained without considering the change in the PSDs found in Area 5 and Area 18.

Conclusion

The 1/d model appears to explain the shape of the specific activity curves of the local fallout particles collected downwind of ground zero. Furthermore, when the ASD is estimated using the 1/d model based on the measured PSD of the soil in the vicinity of ground zero, the measured and predicted fallout patterns also appear to be in excellent agreement. If further research substantiates this model, it may be possible to more accurately predict nuclear fallout detonated in other environments assuming that the PSDs of the soil have been or can be characterized. Additional studies are underway to understand the sources of fractionation affecting the distribution of specific elements, including some fission and fuel products.

Reference

Gregory D. Spriggs et al., "The Activity Size Distribution for Johnie Boy," Lawrence Livermore National Laboratory, UCRL-PRES-227071, August 2008.

Modeling Mix in High-Energy-Density Plasma

by Baolian Cheng and Anthony J. Scannapieco
(Los Alamos National Laboratory)

Material mixing in high-energy-density (HED) plasma governs a wide variety of plasma phenomena in nature, such as supernova explosions, inertial confinement fusion (ICF), and laser ablation. Unlike a normal fluid, HED plasma is a distinct state of matter, containing charged particles (ions and electrons), as shown in Figure 1 (left). Under the influence of a magnetic field, HED plasma may form structures such as filaments, beams, and double layers. Correctly modeling (and perhaps controlling) mixing in ICF capsules and its affect on neutron yield under laser-driven target compression is crucial to ignition studies and other applications.

Mixture in plasma comes in two types: atomic, where the constituents are intimately mixed on an atomic scale, and chunk, where the constituents are in discrete clumps. In hot plasma, the chunks eventually transition into atomic mix. Many leading physicists and mathematicians have been modeling chaotic mixing for decades, with approaches ranging from stochastic models describing the microstructure and evolution of mixing regions to models predicting macroscopic features, such as the growth rate of instabilities and large structures in mixing layers. One effective model for atomic mix in ICF is the multifluid interpenetration mix model developed by Scannapieco and Cheng.[1] This model has shown promise in being predictive for a wide variety of ICF capsules.[2,3]

The multifluid interpenetration mix model was derived from the collisional Boltzmann equation with a particle distribution function in phase space in the presence of external forces. The interactions between species occur through atomic collisions. The rate of change of the distribution function due to collisions is described by the collision term in the equation. In this model, each species has its own pressure, temperature, velocity, energy density and, if necessary, thermal and mechanical stresses.[4] The unresolved component in each dynamic equation (mass, momentum, and energy) is closed by equation-of-state and the collision terms, which are expressed in terms of a single microscopic collision frequency derived from the plasma mean free path, mass densities, interpenetration velocities, and the sound speed in the mixture. The model contains only one free parameter, α, in the phenomenological collision frequency. The parameter is determined by experimental data.

This model has been used effectively to describe atomic mix between fluids and plasmas and yield degradation in capsule performance. In particular, it works well for direct and indirect radiation drive ICF capsules. For example, Figure 1 (middle) shows that setting the sole model parameter, α, to 0.03–0.05 reproduces the yield degradation (relative to clean-burn calculations) with increasing convergence in x-ray driven ICF capsules. The same values of α also capture the yield decrease in direct drive capsules of various wall thicknesses driven with square laser pulses. For thin x-ray driven double shell capsules, the value of the parameter α is found to be 0.05. For thick wall (30 μm) capsules with 15 atm DD fill, the value of α varies slightly over the range 0.05 to 0.07, while for 20 atm DD fill, α ranges from 0.07 to 0.09, as shown in Figure 1 (right). Others have reported the success of this model in explaining the latest ICF experiments by using a small range of α values.[5-7]

The major differences between this and other models lie in the derivations of the model equations, the unique approach to closures, and the number of free model parameters. In contrast to other models, which have several phenomenological parameters for closure, this model introduces only one phenomenological parameter in the collision frequency to characterize the physical system and to describe the unresolved physics at an atomic level. The advantage of doing this is to transform the model approximations from the level of its governing equations to the level of the collision terms, in particular, to a characteristic quantity for binary collisions. This technique enables us to minimize and improve the model approximations through further understanding of the physics of the particle collision process.

Despite the remarkable successes of the model, some important plasma effects are not yet taken into account. Our recent studies indicate that the effects of self-generated electric fields and electron thermal and radiative conduc-

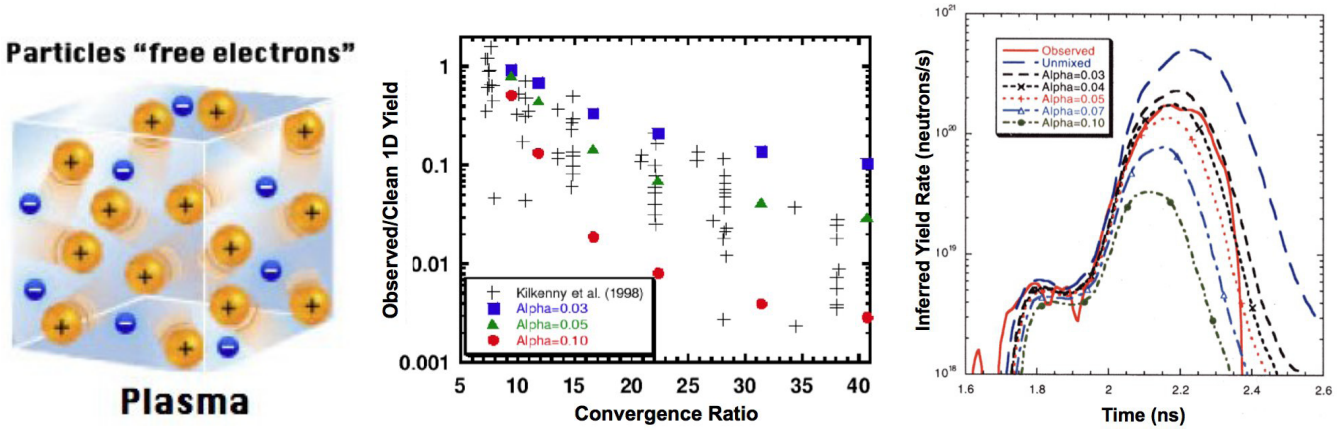

Figure 1. (Left) Illustration of plasma; (middle) yield degradation (relative to clean-burn calculations) in a NOVA experiment and in mixing calculations using α = 0.03, 0.05, and 0.10[2]; (right) observed and simulated neutron temporal diagnostic burn histories for Omega laser shot 25668, both with and without mixing.[3]

tion on the density and temperature of electrons and ions are important in partially ionized plasmas. These effects might not only modify the local electron and ion density distributions, which can be significant in ICF capsules and hohlraum plasmas, but also influence the formation of the hot spots in ICF capsules and affect the burn rate and finally the neutron yield. More recent studies indicate that the plasma effects in the HED regime cannot be neglected.[8-10]

To take plasma effects into account, we have extended the multifluid interpenetration mix model to a partially ionized HED plasma regime and included the effects of self-generated electric fields (from the gradient of electron pressure) and electron thermal conduction. We re-derived the model closures in terms of the physical collision frequency that is uniquely calculated from microscopic physical quantities with no free parameters. Results show that the collision frequency in a partially ionized plasma is enhanced (relative to normal fluids) by ion-ion, electron-ion, and electron-electron collisions. Without ionization, the newly extended model equations reduce to those of the original multifluid interpenetration mix model. We have also added the source terms to the dynamical equations, accounting for the hydrodynamic instabilities directly driven by Rayleigh-Taylor and Richtmyer-Meshkov instabilities. In principle, this newly extended model could describe mix driven by a variety of instabilities depending on the specific form of the external forces. This model can be applied to magnetic confinement fusion when electric-magnetic fields are present and to chemical engineering problems when rotational forces and chemical reaction rates exist. Further verification and validation of this model need to be performed. Its application to National Ignition Facility ignition capsules is under investigation.

References

[1]A.J. Scannapieco and B. Cheng, Phys. Lett. A 299, 49, 2002.

[2]D.C. Wilson et al., Phys. Plasmas 10, 4427, 2003.

[3]D.C. Wilson et al., Phys. Plasmas 11, 2723, 2004.

[4]C.H. Chang and A.J. Scannapieco, LA-UR-12-20777, 2012.

[5]D.C. Wilson et al., Phys. Plasmas 18, 112707, 2011.

[6]J.F. Gu and W.H. Ye., Commun. Theor. Phys. 52, 1102, 2009.

[7]R. Sentis, D. Paillard, C. Baranger, and P. Seytor, European Journal of Mechanics B/Fluid 30, 252, 2011.

[8]K. Molvig, M. Alme, R. Webster, and C. Galloway, Phys. Plasma 16, 023301, 2009.

[9]P. Amendt, O.L. Landen, H.F. Robey, C.K. Li and R.D. Petrasso, Phys. Rev. Lett. 105, 115005, 2010.

[10]B. Cheng et al., in preparation.

The authors thank D.C. Wilson and T.J. Kwan for very helpful discussions, and C.J. Carmer for editing this article.

Quality Input for Microscopic Fission Theory

by Witold Nazarewicz (University of Tennessee/Oak Ridge National Laboratory), Nicolas Schunck (Lawrence Livermore National Laboratory), and Stefan Wild (Argonne National Laboratory)

Soon after its discovery in 1938, Bohr and Wheeler[1] developed the first theory of nuclear fission, a fundamental nuclear process of great relevance to science and society at large. Bohr and Wheeler predicted that significant further theoretical progress would not occur as rapidly because "an accurate estimate for the stability of a heavy nucleus against fission in its ground state will . . . involve a very complicated mathematical problem."[1] Their prognostication has proved true: almost 75 years later, our understanding of this complex phenomenon, involving hundreds of strongly interacting protons and neutrons moving inside a splitting nucleus, remains largely incomplete. There are great expectations, however, that with the help of today's high-performance computers the secrets of fission may finally be unlocked.

Under the Scientific Discovery through Advanced Computing (SciDAC) Univeral Nuclear Energy Density Functional (UNEDF) program[2] and a Stewardship Science Academic Alliances grant,[3] nuclear physicists at the University of Tennessee, Lawrence Livermore National Laboratory, and Oak Ridge National Laboratory, in collaboration with computational mathematicians at Argonne National Laboratory, have recently delivered a validated input for the microscopic description of the fission process in nuclei.[4] The principal goal of this study, which is based on the nuclear density functional theory (DFT) and focuses on the actinide and transactinide regions of the nuclear mass table, is to deliver fission models capable of providing nuclear data not only of a higher quality, but also with quantified uncertainties. For many applications of interest to the NNSA, the required data on fission cross-sections and fission products cannot be obtained experimentally because neutron-rich nuclei with short half-lives are required. Understanding fission— and, in particular, properties of fission fragments—is essential to successfully analyzing fission yields under a variety of conditions and is the starting point for the complex modeling of the prompt fission neutron spectrum. One of the focus areas of the UNEDF fission effort is the development of high-quality input for microscopic fission calculations. Without such input, even the most sophisticated fission approaches based on many-body theory would not be able to produce reliable results. Verified and validated theoretical input is crucial for interpreting experimental data, assessing the importance and feasibility of planned measurements, predicting nuclear properties in the regions that are impossible to access experimentally, and defining future research directions.

The quality of a DFT calculation relies on the form and parameterization of an underlying energy density functional. Since the functional's parameters cannot be derived or computed, they must be optimized based on experimental data. A previous study[5] employed advanced optimization algorithms and high-performance computing to carry out a state-of-the-art optimization of the functional; the resulting parameterization UNEDF0 yields good agreement with experimental masses, radii, deformations, and other global nuclear properties. Recently, in order to develop a high-quality functional for fission, this study was extended by adding excitation energies of fission isomers (superdeformed states on the path to fission) in four actinide nuclei.

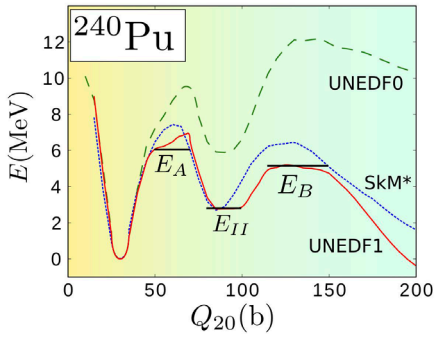

Figure 1. Fission pathway for ^{240}Pu along the mass quadrupole moment calculated with the SkM*, UNEDF0, and UNEDF1 energy density functionals. E_{II}, E_A, and E_B denote the experimental energy of the fission isomer and the inner and outer barrier heights, respectively.

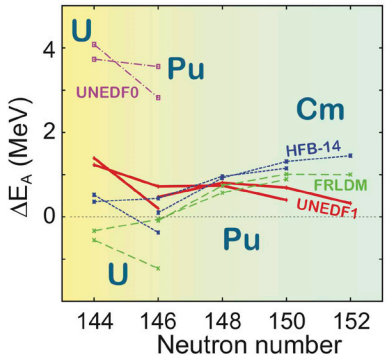

Figure 2. Difference between theoretical and experimental inner fission barriers in U, Pu, and Cm nuclei for the UNEDF0 and UNEDF1 functionals, and FRLDM and HFB-14 models; see reference 4 for details.

A striking feature of the new functional UNEDF1[4] is its ability to reproduce the empirical fission barriers in the actinide region listed in the Reference Input Parameter Library at the International Atomic Energy Agency.[6] As seen in Figures 1 and 2, the quality of UNEDF1 predictions for inner and outer fission barriers is comparable to that obtained in more phenomenological models.[6] Furthermore, UNEDF1's new status as the input of choice when it comes to the microscopic study of the nuclear fission process sacrifices little. Indeed, UNEDF1 provides a description of global nuclear properties that is almost as good as that of UNEDF0. Researchers are encouraged by the finding that deformation properties of the functional can be well-constrained by including only a handful of data relevant to fission. Although the quest for the microscopic fission theory is far from over, a crucial milestone towards this lofty goal has been reached.

References

[1]N. Bohr and J.A. Wheeler, "The Mechanism of Nuclear Fission," Phys. Rev. 56, 426, 1939. http://dx.doi.org/10.1103/PhysRev.56.426

[2]Towards a Universal Nuclear Energy Density Functional, a SciDAC project funded by the DOE's Office for Advanced Scientific Computing Research, Office of Nuclear Physics, and the National Nuclear Security Administration. http://unedf.org

[3]Theoretical Description of the Fission Process, a project supported by the National Nuclear Security Administration under the Stewardship Science Academic Alliance Program through DOE grant DOEDE-FG52-09NA29461. http://www.phys.utk.edu/witek/fission/fission.html

[4]M. Kortelainen, J. McDonnell, W. Nazarewicz, P.-G. Reinhard, J. Sarich, N. Schunck, M. Stoitsov, and S. Wild, "Nuclear Energy Density Optimization: Large deformations," Phys. Rev. C 85:024304, 2012. http://prc.aps.org/abstract/PRC/v85/i2/e024304

[5]M. Kortelainen, T. Lesinski, J. Moré, W. Nazarewicz, J. Sarich, N. Schunck, M.V. Stoitsov, and S. Wild, "Nuclear Energy Density Optimization," Phys. Rev. C 82:024313, 2010. http://dx.doi.org/10.1103/PhysRevC.82.024313

[6]R. Capote et al., Reference Input Parameter Library (RIPL-3), Nucl. Data Sheets 110, 3107 (2009). http://nucleus.iaea.org/CIR/CIR/ReferenceInputParameterLib.html

John Maenchen Named as IEEE Fellow

John Maenchen, Sandia National Laboratories' representative on the NNSA Defense Programs Science Council, has been named as an Institute of Electrical and Electronics Engineers (IEEE) Fellow. Maenchen is being recognized for leadership in the development of intense pulsed charged particle beams and their application for flash radiography.

"This award is well-deserved recognition for John Maenchen's leadership in science, technology, and effects of nuclear weapons through a continuing study and use of plasma physics," said Don Cook, NNSA's Deputy Administrator for Defense Programs. "Being named an IEEE Fellow is a tremendous honor and demonstrates John Maenchen's extraordinary accomplishments. NNSA is fortunate to have dedicated professionals who are truly leaders in their fields working to promote our nuclear security agenda."

The IEEE grade of Fellow, the highest grade of membership, is conferred by the IEEE Board of Directors upon a person with an outstanding record of accomplishments in any of the IEEE fields of interest. The total number selected in any one year cannot exceed 1/10th of 1% of the total voting membership. This year, Maenchen is one of the 321 individuals selected for the prestigious honor and career achievement.

Maenchen received a Ph.D. in ElectroPhysics from Cornell University in 1983 and immediately joined Sandia National Laboratories. As both a scientist and manager he advanced science, technology, and engineering through the design and construction of pulsed power accelerators, the invention and development of new intense electron-beam, ion-beam, and z-pinch loads, the modeling and theory of their operation, the invention of diagnostic approaches to investigate their performance, and the invention and development of new government and commercial applications for these capabilities.

Fiber Reinforced Composites Under Pressure: A Case Study in Non-hydrostatic Behavior in the Diamond Anvil Cell

by Matt Armentrout (Carnegie-DOE Alliance Center (CDAC), Carnegie Institution of Washington)

In high pressure research, a common question is how material properties change as they transition from ambient to extreme conditions. One tool for looking at materials at extreme conditions is the diamond anvil cell (DAC) coupled with synchrotron-based x-ray diffraction. A DAC allows static high pressure to be applied to sub-microgram scale samples up to greater than 100 GPa. X-ray diffraction allows determination of structure and lattice strain within the diamond cell. Many experiments in the diamond cell involve polycrystalline samples with multiple phases coexisting within the cell. If these phases have disparate elastic moduli, the strains experienced by each phase are interrelated.[1] In order to interpret measurements made on such composites in the DAC, we need a better understanding of the physics involved. We are interested in looking at the behavior of mechanical composites at high pressures and temperatures, in order to better understand the partitioning of stress and strain under extreme conditions.

Metal matrix composites (MMC) are a class of high performance materials that are of significant interest from an engineering perspective as a way to reinforce a light material with a strong material. We recently performed experiments on a MMC in the DAC in order to measure stress and strain partitioning on a micromechanical level. Our sample has an aluminum matrix shot through with oriented fibers of ceramic Al_2O_3 (see Figure 1). Aluminum metal is less compressible than Al_2O_3, so the assumption is that it will always strain more under loading. A reasonable aggregate model for a fiber composite is an isostress reaction (Reuss limit) when stressed against the fiber direction, and isostrain (Voight limit) when stressed in the fiber direction. As might be expected the lowest compressibility is along the fiber direction and the highest is against the fiber. This model is broadly consistent with ambient ultrasonic measurements.[2] We performed x-ray diffraction measurements of the composite at high pressures and observed the strain of the component phases both with and against the fibers. Interestingly, our observations are the opposite of our expectations. Against the fibers aluminum and Al_2O_3 are stressed similarly as predicted. However, in the fiber direction Al_2O_3 is stressed considerably less than aluminum. In effect, the direction that is predicted to be strongest at ambient conditions is supporting the least stress at high pressure.

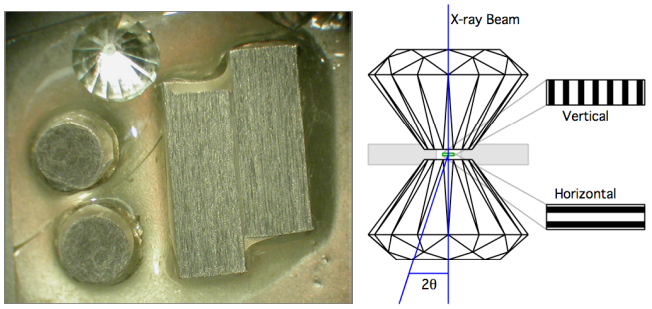

Figure 1. (Above) Parallel and perpendicular slices of the Al_2O_3 composite material, with a 300 mm culet diamond shown for scale. These sections were polished to ~10 μm thick and used as starting materials for the experiments. (Right) Experimental geometry. Composites were aluminum metal infiltrated with oriented Al_2O_3 fibers. Two experiments were run, one with the fibers oriented parallel to the diamond axis and one with the fibers perpendicular. Measurements of lattice strain were performed using x-ray diffraction parallel to the diamond axis only.

An indirect result of the measurement is a lower bound on the yield strength of Al_2O_3. The yield strength marks the transition between reversible (elastic) and irreversible (plastic) deformation. Our lower bound on this strength is the difference between the minimum and maximum inferred stress. In the case of Al_2O_3, we observe an increase in differential stress up to ~10 GPa at a hydrostatic pressure of 20 GPa. Above 20 GPa, we observe a monotonic decrease with increasing pressure.

References

[1]N. Conil and A. Kavner, J. Phys. Condens. Matt. 18, S1039 (2006).

[2]J.E. Vuorinen et al., J. Accoust. Soc. Am. 108, 574 (2000).

Emission of Shocked Inhomogeneous Materials

by Kathryn E. Brown and Dana D. Dlott (CDAC, Carnegie Institution of Washington)

Materials with microstructured inhomogeneities do not necessarily behave under shock compression as their macroscopic parameters, such as particle velocity, Up, would suggest. Time-resolved emission of embedded nanoprobes can give insight into the local response of shocked mesoscale materials. We can selectively attach nanoprobes, including dyes and quantum dots, to different constituents of mesoscale materials, such as molecular crystals (e.g., crystalline explosives), metal particles, or polymer binders (e.g., estane). The nanoprobes are sensitive to both pressure and temperature, and the spectral changes due to shock compression can be compared to those due to static compression and controlled heating in a diamond anvil cell. We developed an apparatus that simultaneously measures macroscopic particle velocity using a homemade displacement interferometer, as well as obtains spectral information on the nanosecond timescale of a shocked inhomogeneous material. As a model system, we shocked a thin film of poly(methyl methacrylate) (PMMA) doped with a rhodamine dye (R640) with a laser-driven flyer plate using a commercial, table-top, Nd:YAG flyer launching system. These kinds of Nd:YAG systems are useful for shock experiments due to their high repetition rate and their ability to be synchronized to a variety of spectroscopic instrumentation. We probed the R640 fluorescence with a doubled Nd:YLF (532 nm) and collected the time-resolved emission with a streak camera and spectrograph.

Laser-driven flyer plates are a convenient tabletop source for shock compression created by high-velocity impact.[1,2] A high energy Nd:YAG (1064 nm) is incident upon a metal foil

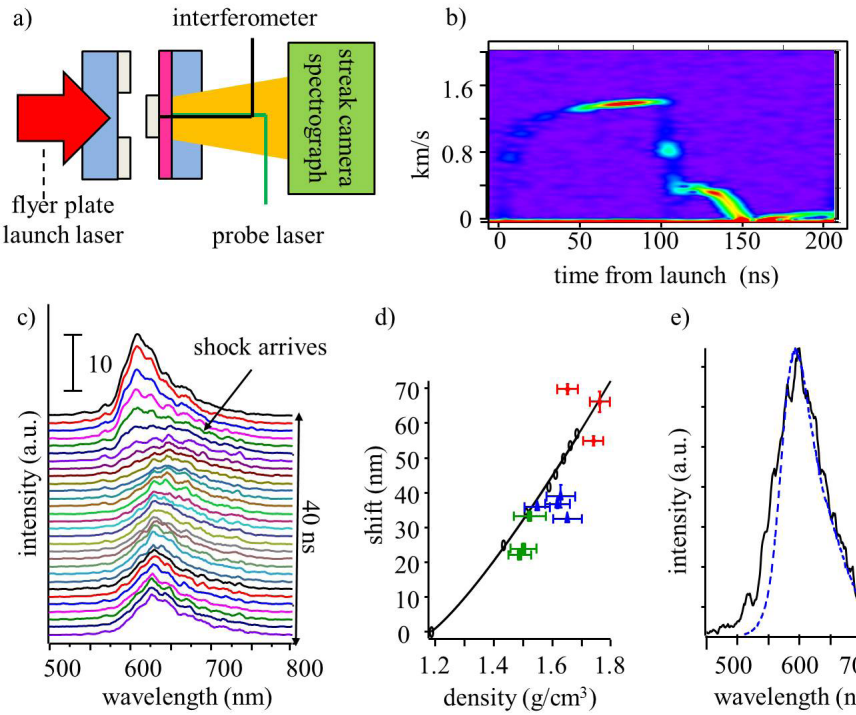

Figure 1. (a) Schematic of shock apparatus. (b) Velocity history of a flyer plate launched to 1.4 km/s and dropped to Up = 0.8 km/s to create a 3.7 GPa shock in PMMA (1.55 g/cm³). Colors indicate intensity of interference fringes (not shown). (c) Time stream of dye emission spectra obtained from streak record. (d) Fluorescence shift vs. density of R640/PMMA in DAC (circles) and under shock from flyer plates traveling at 1.7 km/s (red diamonds), 1.4 km/s (blue triangles), and 0.9 km/s (green squares). (e) R640 fluorescence at peak shock from 1.4 km/s (1.55 g/cm³). Dashed line is DAC spectra at 1.51 g/cm³.

and ablates a portion of it, creating a plasma, which rapidly expands as it absorbs more laser energy. The plasma launches the remainder of the foil across a gap, where it shocks the material of interest. The flyer substrate and target are held in a vacuum chamber. A schematic of the experimental setup is shown in Figure 1a. One challenge with laser-driven flyer plates is the requirement that the drive laser have a top-hat beam profile for flat, intact flyers.[3] We used a newly developed diffractive beam homogenizer and an aspheric bestform lens to obtain a flat-top beam at the foil surface. We have launched aluminum flyer plates that have terminal velocities up to 4 km/s. The thickness of the foil can be varied so that our shock duration is 8-16 ns.

The target can be any material that can be layered on a glass plate. To do simultaneous velocity and spectroscopic measurements, the material needs to be transparent at the interferometer wavelength (1550 nm). Our target sample consisted of a PVA-coated glass plate, with a thin layer of R640/PMMA. R640 was chosen for this preliminary study due to its high quantum yield, short lifetime, and emission wavelength separation from the excitation wavelength. The PVA was used as an impedance-matched cushion, so that the shock was not reflected off of the glass back into the R640/PMMA on our timescale.

The flyer velocity following impact, measured by an interferometer, was used as the particle velocity of PMMA (see Figure 1b). The particle velocity was related to pressure and density using the Hugoniot relation for thin-film PMMA.[4] In order to calibrate the time-resolved fluorescence from our shocked sample (see Figure 1c), we used a diamond anvil cell to collect fluorescence information from a small chip of our R640/PMMA film at discrete, static pressures.[5,6]

The emission spectra from the shocked dye give more local information than the global interferometric data alone. The sensitivity to pressure is manifested by a red shift in the emission spectrum. After the flyer plate impacts the material, the velocity, and subsequently the pressure, eventually reaches zero (see Figure 1b). On our time scale, the emission remains red shifted, indicating that the polymer chains remain densified. Because the dye is more sensitive to density than to pressure, the static pressures were converted to density[7] and our shocked emission was compared to the static emission spectrum of the nearest density. The data seems to be consistent with the shocked R640/PMMA reaching a slightly higher density than the statically compressed material with similar spectral shift (see Figure 1d). Additionally, the excess blue-edge intensity from the shocked material is indicative of shock heating (see Figure 1e).

Our preliminary data indicate that embedded fluorescent nanoprobes may function as sensors of the local environments of mesoscale materials.[8] Future experiments will explore the probes' ability to measure shock temperature, as well as use multiple nanoprobes attached to different constituents of microstructured materials.

References

[1]D.L. Paisley, S.-N. Luo, S.R. Greenfield, and A.C. Koskelo, Rev. Sci. Instrum. 79, 023902 (2008).

[2]D.C. Swift, J.G. Niemczura, D.L. Paisley, R.P. Johnson, S.-N. Luo, and T.E. Tierney IV, Rev. Sci. Instrum. 76, 093907 (2005).

[3]S. Watson and J.E. Field, J. Appl. Phys 88, 3859 (2000).

[4]H. Fujiwara, K.E. Brown, and D.D. Dlott, Shock Compression of Condensed Matter—2011, 1426, 382-385 (2011).

[5]K.E. Brown and D.D. Dlott, J. Phys. Chem. C 113, 5751-5757 (2009).

[6]Y. Fu, E.A. Friedman, K.E. Brown, and D.D. Dlott, Chem. Phys. Lett 501, 369-374 (2011).

[7]J.J. Flores and E.L. Chronister, J Raman Spectrosc 27, 149-153 (1996).

[8]K.E. Brown, R. Conner, Y. Fu, H. Fujiwara, and D.D. Dlott, Shock Compression of Condensed Matter—2011, 1426, 1593-1596 (2011).

Technology Readiness Levels (TRLs)

Originally developed by NASA, TRLs are a systematic metric that provides an objective measure to convey the maturity of a particular technology. Numerous government agencies have modified them for use with their technology projects. The DOE TRLs are provided below. For more information, including descriptions of the levels, refer to the *U.S. Department of Energy Technology Readiness Assessment Guide*, DOE Guide 413.3-4.

TRL 1: Basic principles observed and reported.

TRL 2: Technology concept and/or application formulated.

TRL 3: Analytical and experimental critical function and/or characteristic proof of concept.

TRL 4: Component and/or system validation in laboratory environment.

TRL 5: Laboratory scale, similar system validation in relevant environment.

TRL 6: Engineering/pilot-scale, similar (prototypical) system validation in relevant environment.

TRL 7: Full-scale, similar (protypical) system demonstrated in an operational environment.

TRL 8: Actual system completed and qualified through test and demonstration.

TRL 9: Actual system operated over the full range of expected conditions.

2012 NNSA Stewardship Science Academic Alliances Symposium

NNSA hosted another successful Stewardship Science Academic Alliances (SSAA) Symposium this year with its largest attendance to date. Its more than 275 attendees gathered at a new venue, the Grand Hyatt Hotel, in Washington, DC on February 22-23, 2012 to learn about the projects supported by the SSAA Program and National Laser Users' Facility (NLUF) Program, as well as the NNSA-supported grants from the Joint Program for High Energy Density Laboratory Plasmas.

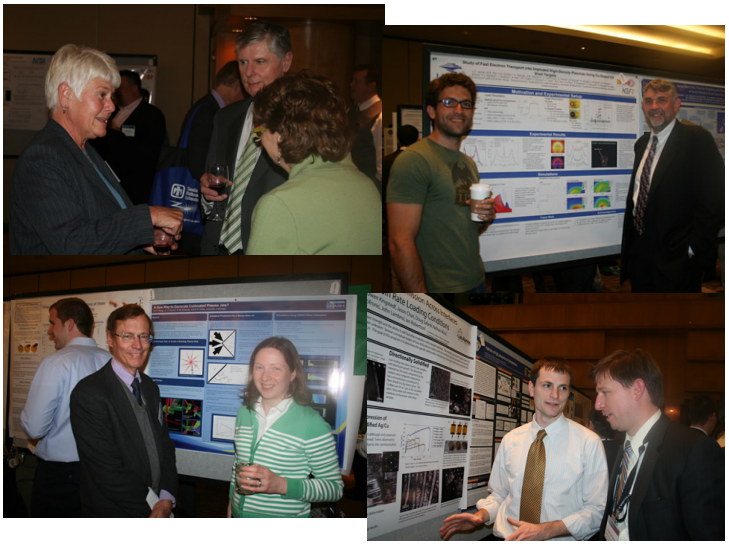

Dr. Chris Deeney, NNSA Assistant Deputy Administrator for Stockpile Stewardship, welcomed the Symposium participants and both reviewed the highlights of the SSAA Program and expressed his hopes for the future of the program. "The phenomenal scientists and engineers we recruit to the SSAA Program ensure its continued success. They are the reason I am confident in our ability to meet the scientific challenges of the future."

Experts in each research discipline presented overview talks. Dr. Jason Burke of Lawrence Livermore National Laboratories (LLNL) kicked off the first day with his introductory overview on nuclear physics entitled "An Overview of Low Energy Nuclear Physics at LLNL and LANL." Dr. John Soures of the Omega Laser Facility at the University of Rochester spoke about the science being done at that facility; his presentation was entitled "High-Energy-Density Physics Research at the Omega Laser Facility."

Two more introductory overviews were presented on the second day of the Symposium. Dr. Todd Ditmire, University of Texas at Austin, discussed the excitement surrounding the field of high energy density science in his talk entitled "The Physics of High Energy Density Plasmas." Dr. Rusty Gray, Los Alamos National Laboratory, followed with a talk describing the problems facing the field of materials under extreme conditions; it was entitled "Material Response Under Extreme Loading Conditions." Approximately 62 talks were presented by grantees during the Symposium.

Dr. Don Cook, the NNSA Deputy Administrator for Defense Programs, delivered the keynote address. His talk, entitled "It's Not Your Grandfather's Deterrent: Looking Backward, Looking Forward," discussed the importance of the scientific work being done from a national security point of view.

The evening's poster session and reception followed the keynote address. The additional space at the venue gave organizers adequate space to display the more than 90 posters. A jury of senior scientists and administrators viewed the posters and voted for outstanding posters in each category. The winners were awarded certificates at the luncheon during the second day.

Organizers selected the Grand Hyatt Washington hotel to accommodate the growing number of attendees. It afforded more space for posters and breakout rooms for the parallel sessions, which allowed the Symposium to be concluded in two days instead of three as in the past. Based on the results of the questionnaire completed by most participants, the change in venue was well received, and participants thought the shorter length and parallel session approach were improvements.

The logistics for the SSAA Symposium were expertly managed by a team from ORISE, led by Tim Ledford. Finally, we owe a debt of thanks to Terri Batuyong, who—once again—worked tirelessly to make the annual SSAA Symposium a success.